International Journal of Earth Sciences Knowledge and Applications
journal homepage: http://www.ijeska.com/index.php/ijeska
e-ISSN: 2687-5993

Research Article https://doi.org/10.5281/zenodo.22163484

Stability Assessment of Rock Slopes at Former Quarries in Singapore

Kar Winn[1,2]*, Chow Weng Lee[3], Ong Perng Fey[4], Htet Aung Linn[5]

[1]Myanmar Geologists Society Singapore, Blk 114, #08-150, Bedok Reservoir Road, Singapore
[2]Newcastle Australia Institute of Higher Education, National Library Building, #13-01 / 02, Singapore
[3]Singapore Professional Engineer (Geotechnical), Singapore
[4]Project Director, Sembcorp Specialised Construction Pte Ltd, 51 Changi Business Park Central 2, #06-12, S486066, Singapore
[5]Senior Manager, Monolithic Pte Ltd, S596692, Singapore

INFORMATION

Article history
Received 12 July 2026
Accepted 20 August 2026
Published 31 August 2026

Contact
*Kar Winn
karwinn@yahoo.com.sg (KW)

How cite
Winn, K., Lee, C.W., Fey, O.P., Linn, H.A., 2026. Stability Assessment of Rock Slopes at Former Quarries in Singapore. *International Journal of Earth Sciences Knowledge and Applications* 8 (2), 202-222. https://doi.org/10.5281/zenodo.22163484.

Abstract
The redevelopment of abandoned quarry sites in Singapore requires precise rock slope stability assessments to ensure public safety. This study evaluated the applicability of the Q-slope and ROFRAQ methods to the Granite of Bukit Timah Centre. The Q-slope method for rock slope engineering was developed to enable engineering geologists and rock engineers to rapidly assess the stability of excavated rock slopes in the field and to make optimal adjustments to slope angles as rock mass conditions become apparent during construction of road cuts or benches. An empirical relationship between Q-slope and long-term stable slope angle is now supported by more than 600 case studies across 36 rock types on five continents. This paper presents the first application of the Q-slope method to abandoned quarry walls in Singapore. In Project 1, the rock slope was prepared for public viewing in its natural condition without artificial support; manual scaling was carried out to remove loose rock blocks. In Project 2, an assessment was conducted to evaluate the suitability of the rock slope for hiking. The study also investigated the relationship between Geological Strength Index (GSI) and Q-slope. Additionally, Rockfall Risk Assessment for Quarries (ROFRAQ), though initially developed for temperate climates, has been validated for use in tropical regions such as Singapore.

Keywords
Q-slope, Stability of rock slope, Scaling work, Slope angle, Geological Strength Index (GSI), Rockfall Risk Assessment for Quarries

List of Symbols

β: Long-term stable slope angle in degrees
CSMR: Continuous slope mass rating
FEM/DEM: Finite element method/Finite difference method
GSI: Geological Strength Index
J_n: Joint sets number
J_r: Joint roughness number
J_a: Joint alteration number
J_{wice}: Environmental and geological condition number
MRMR: Mining rock mass rating (Laubscher, 1977; Laubscher and Jakubee, 2001)
O-factor: Orientation factor for the ratio of J_r/J_a
Q-slope: Empirical method of rock slope stability analysis
Q-slope': Modified Q-slope value that does not consider orientation factors, external factors and stress
RMR: Rock mass rating (Bieniawski, 1976; 1989)
ROFRAQ: Rockfall Risk Assessment for Quarries product of ratings (A to F)
$ROFRAQ_{BASIC}$: Based only on the first four ratings (A-D)
RQD: Rock quality designation
SMR: Slope mass rating

SRF_{slope}: Maximum of three strength reduction factors a, b and c
SRF_a: Physical condition number
SRF_b: Stress and strength number
SRFc: Major discontinuity number

1. Introduction

In the abandoned quarry designated for future recreational use—similar to cases reported in Turkey and Poland (Kalpakci et al., 2016; Kolano et al., 2025) several slope stability concerns were identified. A comprehensive geotechnical and engineering geological assessment was therefore undertaken, including discontinuity mapping, laboratory characterization of rock materials, kinematic evaluation of potential failure modes, and numerical and limit-equilibrium slope stability analyses. Stabilization measures were recommended in line with the analysis results, while also considering case study limitations and environmental constraints.

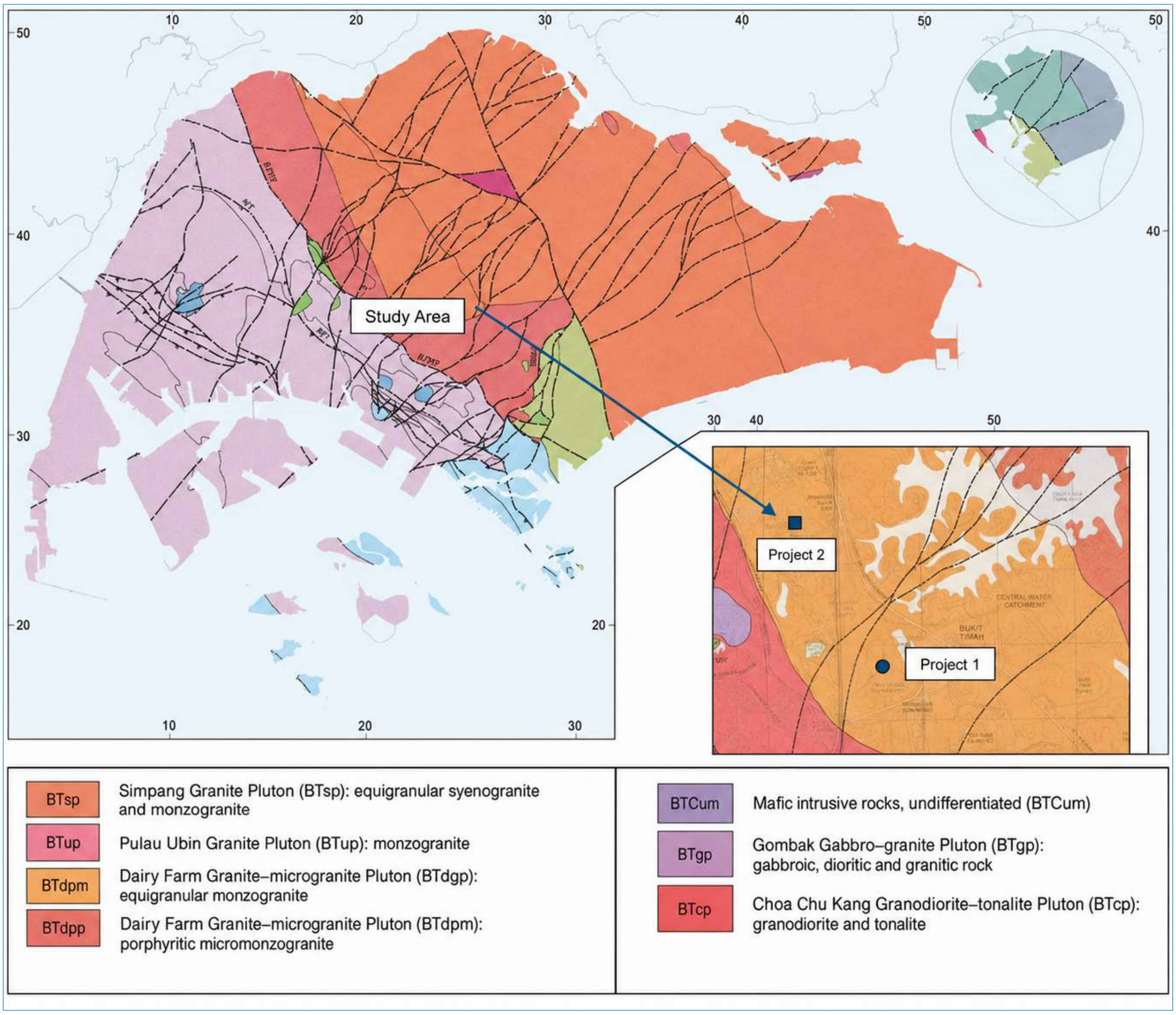

Fig. 1. Geology Map of the Study Area (BCA, 2021)

1.1. Project Background

Singapore's quarrying industry dates back to the 19th century, with large-scale granite and sand extraction intensifying and peaking in the 1960s to meet construction demands. These activities, however, caused significant environmental degradation, as silt- and mud-laden runoff polluted surrounding areas and contributed to landslides and flooding. In response, quarrying operations on mainland Singapore ceased by 1970, while island quarries closed later, with the last ones shutting down in 1991. Today, many former quarry sites have been repurposed into scenic nature parks and recreational areas, while others have been filled with earth or allowed to accumulate rainwater and groundwater, forming lakes and ponds.

In this study, Project 1—Riffle Range Nature Park—was established to protect surrounding nature reserves, whereas Project 2—Dairy Farm Quarry—has become a site for mountain biking and rock climbing. In land-scarce Singapore, post-mining areas such as these are progressively being transformed for public use. Because hard rock quarries are dominated by steep, towering slopes, reclamation approaches must be adapted to their distinct physical characteristics.

Restoration commonly prioritizes natural landscape rehabilitation alongside recreational, educational, and geotouristic functions. When carried out effectively, the redevelopment of post-mining areas enhances both visual appeal and functional value. Consequently, maintaining safe conditions is essential, with slope stability remaining a primary consideration in design and management to minimize risks of slope failures and rockfalls, thereby safeguarding the public and preventing accidents.

1.2. Slope Stability Analysis

In both civil and mining engineering projects, real-time assessment of rock slope and bench stability is rarely feasible using analytical methods such as kinematic analysis, limit-equilibrium techniques, or numerical modelling (FEM/DEM). Excavation typically progresses too rapidly for these approaches to be applied effectively (Bar and Barton, 2017).

Over the past 50–60 years, numerous empirical methods have been developed to support rock engineering design, and these are now widely applied across civil and mining projects. In tunnelling, underground mining, and other subsurface excavations, several established empirical systems are routinely used to determine appropriate support and reinforcement measures for given excavation spans, including:

- Q-system (Barton et al., 1974; Barton and Grimstad, 2014)
- RMR: Rock Mass Rating (Bieniawski, 1976, 1989)
- MRMR: Mining Rock Mass Rating (Laubscher, 1977; Laubscher and Jakubee, 2001)

In assessing rock slope stability, empirical approaches were seldom applied; instead, practitioners often relied on simple kinematic analyses, numerical modelling, or, in some cases, no formal modelling at all—where slope angles were determined by equipment operators or foremen rather than engineers. SMR (Slope Mass Rating) and CSMR (Continuous Slope Mass Rating) were developed to predict the support, reinforcement, and performance of excavated slopes (Romana, 1985; Romana, 1995; Tomas et al., 2007; Tomas et al., 2012).

However, no empirical rock engineering methods currently provide guidance on determining suitable, long-term stable slope angles where reinforcement and support are intentionally excluded. Yet such unsupported slopes represent the majority of practical demand. The Q-slope method, introduced in 2015, was designed to help engineering geologists and rock engineers evaluate the stability of excavated rock slopes directly in the field and adjust slope angles as rock mass conditions become apparent during construction (Barton and Bar, 2015; Bar and Barton, 2017; Bar and Barton, 2025).

Fig. 2 Porphyritic granite of Dairy Farm Granite-microgranite Pluton (BTdpm): a) Core samples showing Total core recovery (TCR), Solid core recovery (SCR) and Rock quality designation (RQD) and b) Close-up photo showing porphyritic texture (BCA, 2021)

Key applications extend from the surface downward, encompassing bench angle determinations in open-pit mines as well as slope excavations required for hydropower developments, tunnels, and dam sites—often in terrains characterized by highly variable geological structures.

Each year, tens to hundreds of thousands of kilometres of unsupported rock slopes were constructed for roads, railways, hydropower developments, tunnel and dam access routes, and benches in surface mines and quarries. In most cases, slopes were excavated through variable geological conditions with changing lithologies, weathering profiles, and discontinuities.

Excavation frequently leads to problematic and potentially hazardous local failures, often caused by adverse plane failures, wedge failures, or, less commonly, local toppling. Complex interactions between these mechanisms may arise, sometimes accompanied by shearing through weak rock masses. Applying the Q-slope method can minimize maintenance requirements (including bench-width demands) by addressing potential failure mechanisms, while also enhancing safety through reduced slope failures linked to human activity.

Over the past decade, several investigators have developed and validated modifications to the Q-slope classification system to increase predictive accuracy and adapt it for diverse geological settings (Azarafza et al., 2020; Kouhdaragh et al., 2022; Mao et al., 2023). Gupta et al. (2025) developed an open-source, multi-platform application known as the Q-slope Calculator to streamline Q-slope–based rock slope stability assessments. The tool incorporates both manual and automated computation workflows and was implemented along a geologically vulnerable stretch of National Highway-7 (NH-7) between Karnaprayag and Joshimath in the Lesser Himalayas.

In Project 1, a monzogranitic rock slope approximately 30 m high in an abandoned quarry—severely damaged by drill-blast operations—was assessed. The slope is intended to support a public viewing deck at the cliff top, allowing visitors to appreciate the natural features of the rock face.

As visible artificial support was not preferred, the required slope angle for long-term stability was determined using the Q-slope method. The application of this methodology is presented in the following sections. Similarly, for Project 2, an assessment was conducted to evaluate the suitability of the rock slope for hiking.

While the Q-slope method has been validated across more than 600 case studies globally, its application to the unique tropical weathering profiles of Southeast Asia—specifically the Bukit Timah Centre Granite in Singapore—remains unexplored. This study addresses this gap by providing the first empirical evidence of Q-slope's efficacy in Singapore's highly weathered and jointed granitic rock masses. Unlike studies in temperate regions, this research accounts for the intense chemical weathering and high-intensity rainfall characteristic of tropical environments, establishing a novel correlation between Q-slope and the Geological Strength Index (GSI) (R^2 = 0.922).

1.3. Rockfall Analysis

Research on rockfalls in quarries has historically been less extensive compared to studies in road cuts, mountainous terrain, and open-pit mines. This is largely because road cuts and mountain slopes often pose direct hazards to public safety (drivers, hikers, and nearby communities), whereas quarries are typically controlled industrial sites with restricted access.

Alejano et al. (2008) proposed an empirical method, Rockfall Risk Assessment for Quarries (ROFRAQ), designed to evaluate the risk associated with rockfalls in hard rock quarries and open-pit mines. The method is inherently probabilistic, recognizing that accidents arise not from isolated factors but as the outcome of a sequence of interrelated events.

Fig. 3. The old quarry wall slope (Project 1)

Table 1. Joint system of the rock mass (Project 1)

Joint set	Dip amount/Dip direction
1	70 / 320-330
2	35 / 240-255
3	50 / 60-75

Although originally developed using data from Galician rock quarries in northwestern Spain under temperate climatic conditions, the method has proven applicable to tropical environments such as Singapore. Local climatic factors, particularly rainfall intensity and seasonal variability, may influence slope behaviour; however, the probabilistic framework and guideline-based nature of ROFRAQ allow it to be adapted effectively across diverse geological and climatic contexts.

The method is based on the observation that rockfall-related accidents in mining environments typically occur as a consequence of six sequential events known as ratings for assessment:

- A detached block or rock mass exists on a slope (A).
- The block or rock mass is close to equilibrium (under a given instability mechanism) (B).
- A triggering phenomenon renders the block or rock mass unstable ‘(C).
- The fall path allows one or more blocks to reach the quarry bottom (D).
- At least one block impacts a worker or machine ‘(E)
- Quarry rockfall history (F)

The product of these factors (A to E), combined with a corrective value based on the quarry’s rockfall history (rating F in the proposed method), yields the ROFRAQ index, which provides a yearly estimate of the likelihood of a rockfall-related accident occurring on a given quarry slope. Sensitivity analyses indicate that rating E—the likelihood of a falling block striking a worker or machine—is the most significant factor. To measure the likelihood of a rockfall occurring irrespective of the final outcome (accident or no accident), a simplified version of the index, $ROFRAQ_{BASIC}$, is proposed, based only on the first four ratings (A–D). Kolano et al. (2015) investigated the stability of rock slopes in a former limestone quarry in Poland through literature review, field investigations, and stability analyses. Their study demonstrated that FEM numerical slope stability calculations with explicitly modelled discontinuity networks not only identified realistic failure mechanisms but also produced accurate values of stability indicators.

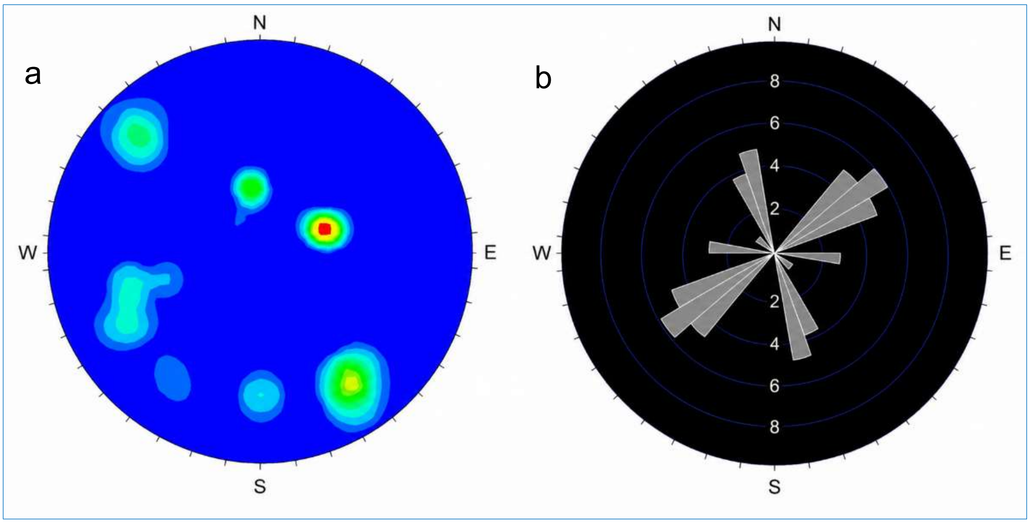

Fig. 4. a) Contour diagram of joint system of the rock mass and b) Rose Net diagram of joint system. (3 major joint sets with a few minor set) (Project 1)

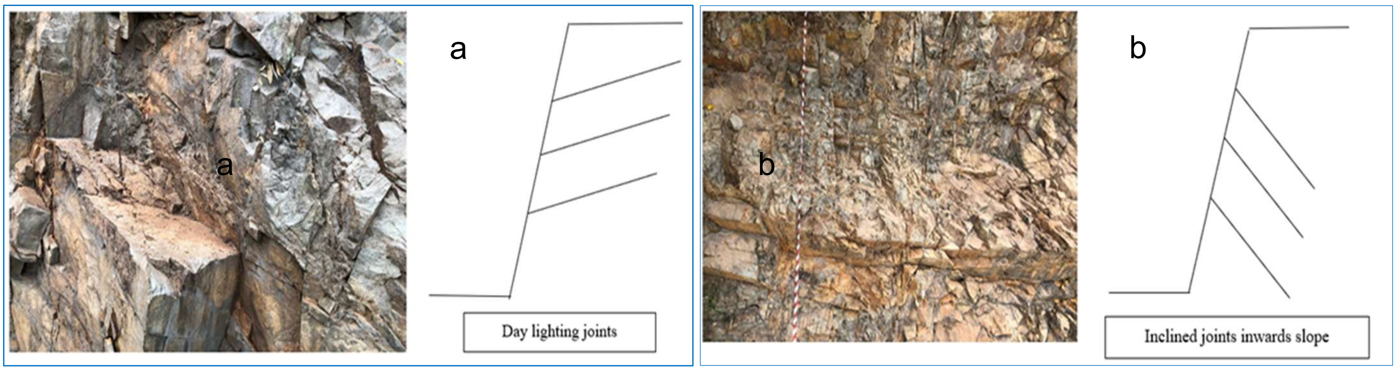

Fig. 5. a) Some noticeable joint system of rock mass, day lighting joint (Project 1) and b) Inclined inward joint (Project 1)

1.4. Climatic Condition of Singapore

Singapore has a tropical rainforest climate due to its location near the equator. The climate is characterized by consistently high temperatures, high humidity, and abundant rainfall throughout the year, with minimal seasonal temperature variation.

1.4.1. Key Climate Characteristics

- Average annual rainfall: approximately 2,113 mm/year (1991-2020 climatological average).
- Rainy days: approximately 171 days per year.
- Temperature: generally, ranges from 24°C to 32°C throughout the year.
- Relative humidity: typically exceeds 80%.

1.4.2. Rainy Seasons (Monsoon Periods)

Singapore experiences two main monsoon seasons separated by inter-monsoon periods:

- Northeast Monsoon (December to early March): generally, the wettest period of the year, with frequent and prolonged rainfall events. .

- Southwest Monsoon (June to September): relatively drier but still experiences short-duration thunderstorms and occasional Sumatra squalls.

Inter-monsoon periods (March to May and October to November): characterized by intense afternoon and evening thunderstorms.

1.4.3. Impact on Slope Stability in Singapore

Singapore's tropical climate significantly influences slope performance and geotechnical stability:

- Increased pore-water pressure: Heavy and prolonged rainfall infiltrates into slope materials, increasing pore-water pressure and reducing effective stress and soil shear strength, which can lead to slope instability or failure.
- Reduction of matric suction: Many soil slopes in Singapore comprise residual soils derived from the granitic and sedimentary bedrocks. These partially saturated soils rely on matric suction for additional shear strength. Prolonged rainfall reduces matric suction, thereby decreasing slope stability.
- Surface erosion: Intense rainfall can cause surface erosion, loss of vegetation cover, and degradation of the slope surface, progressively weaken the slope and increase susceptibility to failure.

2. Geology of the Project Area

The geological history of Singapore is dominated by Mesozoic events associated with the evolution of the Sukhothai Arc and two Palaeozoic continental fragments (Indochina-East Malaya and Sibumasu) that rifted separately from Gondwana then amalgamated with the arc to form Mesozoic Sundaland. The Bukit Timah Fault Zone (BTFZ), a large and long-lived fault, effectively divides Singapore into two main parts, each representing a different component of the arc history. Arc-related Permian and Triassic plutons of the Bukit Timah Centre (BTC) crop out on the north-east side of the fault, often concealed beneath the Cenozoic sediments and sedimentary strata deposited in the forearc basin crop out exclusively on the south-west side of the BTFZ. The central and eastern parts of Singapore are underlain predominantly by granitic to gabbroic rocks of the BTC, a Permian–Triassic plutonic igneous complex that occupies approximately three-fifths of mainland Singapore (BCA, 2021). The Building and Construction Authority's (BCA) deep ground investigation programme has identified this complex as a world-class example of I-type pluton architecture. Based on lithological distinctions, the BTC is subdivided into five plutons namely Choa Chu Kang Granodiorite-tonalite Pluton, Gombak Gabbro-granite Pluton, Dairy Farm Granite-microgranite Pluton, Pulau Ubin Granite Pluton and Simpang Granite Pluton.

Table 2. Q-slope and β determination of quarry wall rock mass (Project 1)

Parameter	Case 1 (Area with free of loose rock pieces)	Case 2 (Area with loosely attached rock pieces)
RQD	90	90
J_n	12	12
J_r	2	2
J_a	1	1
O factor	1	0.75
J_{wice}	0.7	0.7
SRF_a	2.5	2.5
SRF_b	1	2.5
SRF_c	1	2
Q-slope	4.2	0.63
β (Slope angle)	77	61

2.1. Dairy Farm Granite-Microgranite Pluton

Both study areas belong to the Dairy Farm Granite–Microgranite Pluton of the Bukit Timah Centre (BCA, 2021), as shown in Fig. 1. All parts of this pluton are of monzogranite composition; however, the unit comprises two texturally distinct components. The western sector is dominated by inequigranular (porphyritic) textures, whereas the eastern sector is entirely equigranular. The two projects examined in this study are in the western sector.

In the best-developed examples of the inequigranular rocks (Fig. 2), phenocrysts of plagioclase, alkali feldspar, biotite, and quartz, together with fragments of plagioclase-rich rock, are set within a quenched groundmass of very fine, equigranular quartz and feldspar. The granitic rock is a holocrystalline, fine to medium grained, leucocratic showing a predominantly pink to white colour and phaneritic with some dark particles, possibly biotite.

Most grains are angular to subrounded in shape. The rock mainly consists of quartz which is identified as a glassy colourless mineral and feldspar which is identified as pink and white mineral. Generally, the rock consists of macro quartz (30-35%), orthoclase feldspar (35%), Plagioclase feldspar (20%) with biotite (10%).

A sample of monzogranite from this pluton yielded a zircon population with a U-Pb age of 244 ± 2 Ma (BCA, 2021). Four previously reported U-Pb zircon ages expand the age range for the pluton to approximately 246–235 Ma.

The rock is observed in a slightly weathered condition and is highly jointed (Fig. 3). The slope under stability study is an abandoned quarry wall where rocks were mined by drill-and-blast methods for construction purposes.

2.2. Brittle Deformation of Timah Centre (BTC)

The granitic rocks of the BTC are transacted by an array of predominantly north-northeast to south-southwest–trending brittle faults. These faults generally exhibit relatively straight traces, suggesting steeply dipping to subvertical geometries. Brittle deformation leading to faulting has played a critical role in the geological evolution of Singapore and represents a major control on the subsurface distribution of lithological units. The Bukit Timah Fault Zone (BTFZ), shown in Fig. 1, is the largest and arguably the most significant structural discontinuity in Singapore. It delineates the boundary between the plutonic rocks of the BTC and the sedimentary and volcanogenic strata in the southern and southwestern parts of the island.

2.2. Brittle Deformation of Bukit Timah Centre (BTC) Granite

Owing to Singapore's tropical climate, the country's bedrock is subjected to intense physical and chemical weathering. Consequently, the general geology of the Bukit Timah Centre Granite can be described by a three-layer model comprising:

- A thick residual soil layer (Weathering Grade VI)
- Moderately weathered granite (Grade III)
- Slightly weathered to fresh granite bedrock (Grades II–I)

Generally, between three to five sets of discontinuities are recognised in both BTC and sedimentary rocks in the country with the dominant sets appearing to be subvertical and striking north-north-west to south-south-east, north-north-east to south-south-west. More gently inclined joints and north-south and east-west-striking sets are also reported, though less frequently. Overall, joints are expected to decrease in frequency and aperture with depth below the present land surface.

Dense jointed strips commonly occur within the rock mass (Figs. 3, 5 and 11). These structures are generally subvertical and randomly distributed, with variable spacing between adjacent strips. Rock mass permeability at the site is relatively low, as evidenced by minimal groundwater seepage observed on slope faces in the projects.

3. Stability Assessment of Rock Slopes for Former Quarries at Project 1 (Field Assessment and Manual Scaling Works)

The slope stability assessment was conducted during major construction works (Winn et al., 2022). Using a boom lift (Fig. 3), the entire surface condition of the rock slope was evaluated. Geological structures (discontinuities within the rock mass) were measured, and the required engineering geological parameters were recorded for further analysis. The current rock slope faces southwest, with an orientation of approximately 070/240–250, an inclination of ~70°, and a height of 30 m.

Fig. 6. a) and b) Observed loosely attached rock pieces on different locations on rock slope (Project 1)

3.1. Joint (Discontinuity) Systems of the Rock Mass

The lithology of the quarry wall is monzogranite igneous rock, commonly exhibiting a porphyritic texture. The dip amount and direction of joint planes were measured using a geological compass by the sighting method during fieldwork. Three major joint sets, along with a few minor sets, were observed (Table 1). A stereographic projection of the joint systems, generated using the Dips program, is shown in Fig. 4. Among these joint sets, two types are particularly significant:

- Daylighting joints – inclined outward from the slope face (Fig. 5a).
- Inward-inclined joints – dipping into the slope face (Fig. 5b).

3.2. Stability Analysis of Quarry Wall Slope by Empirical Q-slope

Barton and Bar introduced the Q-slope method at the Eurock 2015 (European Rock Mechanics) Conference, with further notes presented at the ARMA 2016 Symposium. Q-slope enables geotechnical engineers and engineering geologists to rapidly assess slope stability in the field, both during and after excavation (Barton and Bar, 2015; Barton and Bar, 2019; Barton et al., 2018; Bar and Barton, 2016; Bar and Barton, 2017; Bar and Barton, 2018a; Bar and Barton, 2018b; Bar and Barton, 2025).

For Q-system users, the formula for estimating Q-slope is mostly familiar (Barton and Bar, 2015).

$$Q - slope = \left(\frac{RQD}{J_n}\right) \times \left(\frac{J_r}{J_a}\right)_O \times \left(\frac{J_{wice}}{SRF_{slope}}\right) \quad (1)$$

The rating system of each parameter (RQD, J_n, J_r, J_a, J_{wice} and SRF_{slope}) in *Equation 1* is given in the Appendix Section of paper by Barton and Bar (2015) and Bar and Barton (2016). The Q-slope method requires the assignment of ratings for rock quality designation (RQD), joint set number (J_n), joint roughness number (J_r) and joint alteration number (J_a), which remain unchanged from the original Q-system (Barton et al. 1974).

For Q-system users, *Equation 1* for estimating Q-slope is mostly familiar (Barton and Bar, 2015; Barton and Bar, 2015; Barton and Bar, 2019; Barton et al 2018; Bar and Barton, 2016; Bar and Barton, 2017; Bar and Barton, 2018a; Bar and Barton, 2018b; Bar and Barton, 2025).

Barton and Bar (2015) derived a simple formula for the steepest angle (β) not requiring reinforcement or support for slope:

$$\beta = 20 \log_{10} Q\text{-slope} + 65° \quad (2)$$

The recorded and calculated Q-slope values, along with maximum stable slope angles for two scenarios, are presented in Table 2. Engineering judgment was applied in these empirical approaches, based on the experience of the engineer and local conditions.

- Case 1 (area free of loose rock pieces): The calculated steepest angle (β) is 77°, indicating that the current slope of 70° is stable.
- Case 2 (area with loose rock pieces): The calculated steepest angle (β) is lower than the current slope, indicating instability under long-term conditions.

3.3. Recommended Scaling of Loosely Attached Rock

Loose rock fragments of varying sizes (Fig. 6) were observed at different locations on the slope. These were formed during previous drill-and-blast quarrying operations and remained after incomplete scaling.

Since the natural rock slope face was intended for public viewing, slope protection measures such as shotcrete, rock bolts, or steel mesh were not feasible. For long-term stability and worker safety during future maintenance, it is recommended that loose rock pieces in Case 2 areas (Table 2) be removed manually or mechanically. Special attention should be paid to daylighting joints (Fig. 5a), which are prone to outward failure.

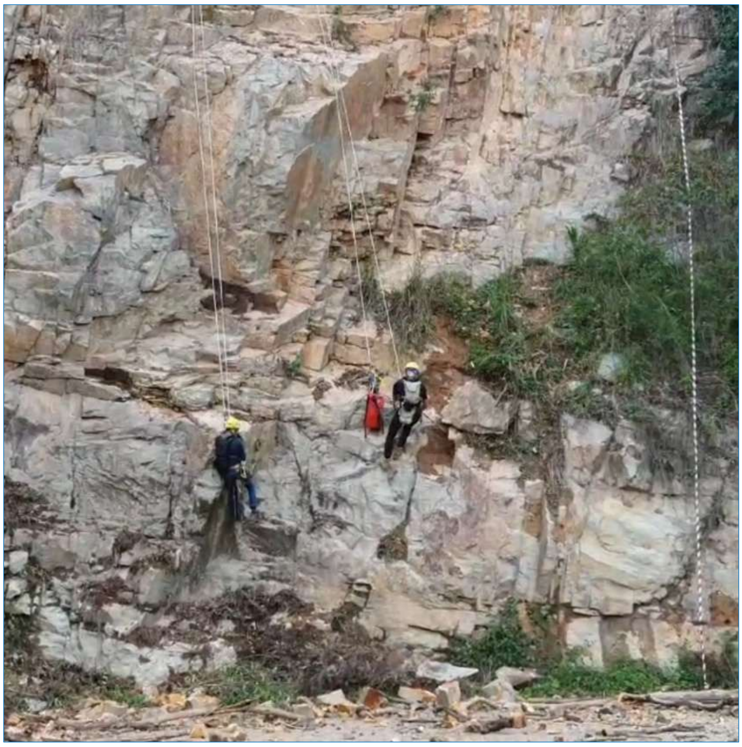

Fig. 7. Manual scaling work (Project 1)

3.4.1. Manual Scaling Works

Scaling was performed by rope-access specialists (Fig. 7). The primary objectives were to remove loose rocks on daylighting joint planes and potential debris to ensure safety and prevent injuries or damage during future works below the cliff. The rock face was systematically scanned multiple times from top to bottom and left to right. Priority was given to areas highlighted during the initial assessment, which were thoroughly checked and scaled down.

3.3.2. Empirical Q-slope Stability Analysis of Quarry Wall Slope After Scaling Work

Following manual scaling, the rock slope face was divided into four zones for final assessment. The recorded and calculated Q-slope values, along with maximum stable slope angles for these zones, are presented in Table 3. For slope areas free of loose rock fragments after scaling, the calculated steepest angle (β) requiring no reinforcement or support ranged between 75° and 84°. This confirms that the current slope of 70° is stable. Comparative photographs of the slope face before and after scaling are shown in Fig. 8. The overall slope condition after scaling, with the Colugo Deck structure installed at the cliff top for public viewing, is shown in Fig. 9. Stabilization measures such as rockfall protection meshes and anchoring systems were not permitted by the authorities. Instead, hazard and protective buffer zones were established to separate visitors from the cliff base, ensuring safe public use of the site. The area was officially launched by the National Parks Board in November 2022, enhancing accessibility to the forest and trails for the public (Winn et al., 2022).

Table 3. Q-slope and β determination after manual scaling (Project 1)

Parameter	Slope face after free of loose rock pieces			
	Zone A	Zone B	Zone C	Zone D
RQD	85	85	95	85
J_n	12	12	12	12
J_r	2	2	2	2
J_a	1	1	1	1
O factor	1	1	2	1
J_{wice}	0.7	0.7	0.7	0.7
SRF_a	2.5	2.5	2.5	2.5
SRF_b	1	1	1	1
SRF_c	1	1.25	1	1.25
Q-slope	3.97	3.2	8.87	3.2
Steepest angle (β) not requiring reinforcement or support	77	75	84	75

4. Stability Assessment of Rock Slopes for Former Quarries at Project 2 (Old Dairy Farm Quarry)

Dairy Farm Quarry (Project 2) comprises abandoned quarry walls where aggregates were mined by drill-and-blast methods for construction purposes. The quarry was backfilled with earth when mining activities ceased in the 1970s–1980s.

Today, the area is popular among climbers and adventure seekers. An engineering geological study was conducted to evaluate the stability of rock cliffs at 20 specified sites within the former quarry. Geological structures (discontinuities in the rock mass) were mapped and measured, and engineering geological parameters visible from the ground surface were recorded. Drone surveys were employed to capture photographs of the upper portions of rock slopes and hilltops for further analysis. The current rock slope faces are oriented east–west, with inclinations exceeding 70°.

The assessment focused on determining whether existing rock-climbing spots at these sites are safe for public use, based on risk-impact evaluation. Recommendations were subsequently provided regarding appropriate actions and improvement measures to ensure park safety.

Fig. 8. Comparison of rock slope condition at some selected locations (Project 1): a) before scaling work and b) fter scaling work

4.1. Joint (discontinuity) Systems of the Rock Mass

Geologically, the study area belongs to the Dairy Farm Granite–Microgranite Pluton of BTC, the same unit as Project 1 (Fig. 1). The dip amount and direction of joint planes were measured using a geological compass by both contact and sighting methods during fieldwork. Three major joint sets, along with several minor sets, were identified (Table 4; Fig. 10).

4.1.1. Modes of Rock Slope Failure

Two types of rock slope failure were observed in the area.

a. Geological structures-controlled rock slope failure (Fig. 11)

- Day-lighting joints-controlled failure (Fig. 11a)
- Sheet joints (exfoliation joints)-controlled failure (Fig. 11b)
- Toppling failure (Fig. 11c)
- Wedge type failure (Fig. 11d)

b. Weathering effect-controlled rock slope failure Fig. 12.

4.1.2. Blast-induced Slope Failure

In addition to above naturally occurring failures, loosely attached rock fragments of varying sizes (Fig. 13) were observed at multiple locations on the slope, like Project 1. These fragments were formed during previous drill-and-blast quarrying operations and remained after incomplete scaling.

4.1.3. Recent Rock Fall During Study Period of June–July 2021

During the field investigation, several rockfalls were observed at specific locations, triggered by heavy rainfall and other natural hazards (Fig. 14).

4.2. Methods of Stability Analysis of Rock Slopes

The base and face of the >30 m-high rock slope are densely vegetated; strictly preserving the natural environment was a paramount constraint. Accordingly, geological structures (discontinuities) were mapped and measured, and engineering geological parameters visible from the slope toe were documented (Fig. 15a). To evaluate the upper reaches of the rock slopes and hilltops in detail without environmental impact, drone imagery was utilized (Fig. 15b).

Fig. 9. Overall rock slope condition after scaling work with colugo deck structure on top (Project 1)

Table 4. Joint System of the rock mass at Project 2

Joint set	Dip amount/Dip direction
1	90/080-260
2	90/180-360
3	50/210

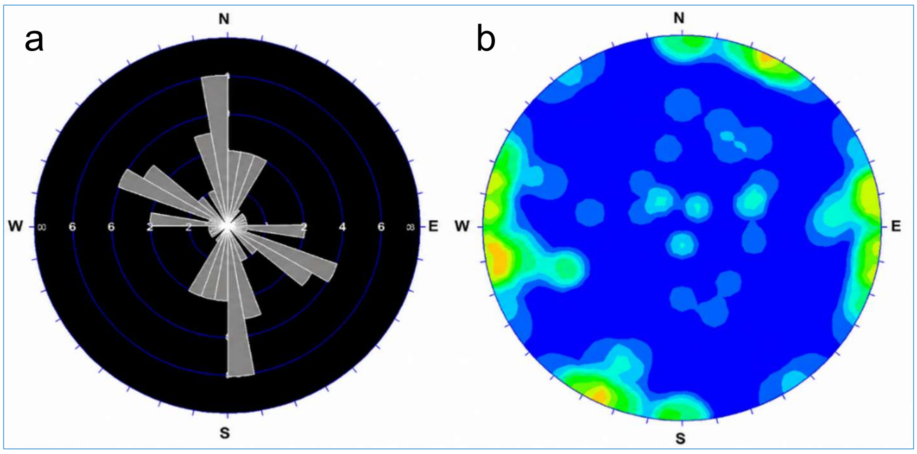

Fig. 10. a) Rose Net diagram of joint system of Project 2 and b) Contour diagram of joint system of the rock mass. (3 major joint sets with a few minor set) (Project 2)

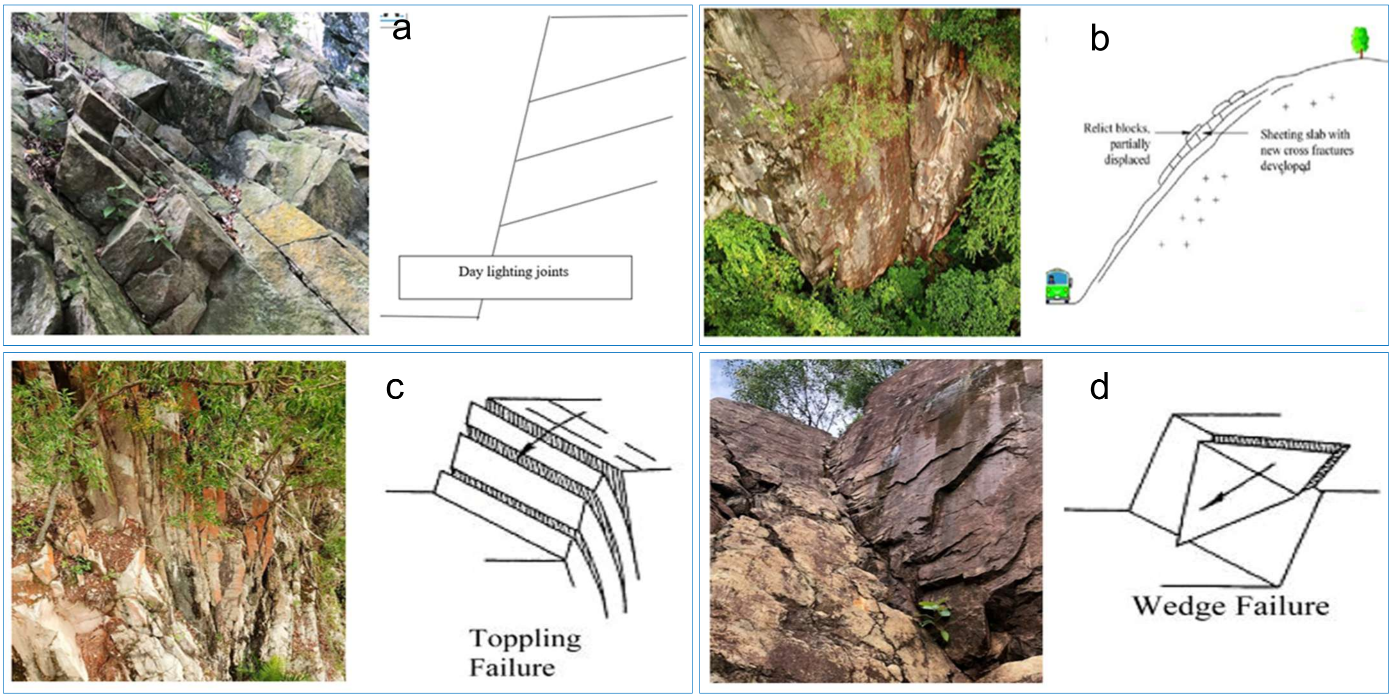

Fig. 11. Types of Geological structures-controlled rock slope failure observed at Project 2: a) Failure by Daylighting joint, b) Failure along sheet joints, c) Toppling failure and d) Wedge failure

Fig. 12. White-coloured loose residual soil falling from slope top (Weathering effect-controlled rock slope failure)

The empirical Q-slope method (Barton and Bar, 2015; Barton and Bar, 2019; Barton et al., 2018; Bar and Barton, 2016; Bar and Barton, 2017; Bar and Barton, 2018a; Bar and Barton, 2018b; Bar and Barton, 2025) was applied, as in Project 1. Physical measurements of geological structures and parameters for Q-slope determination were carried out up to accessible levels from the slope base. Drone photographs of the upper slope levels were integrated to provide a comprehensive assessment of the entire area.

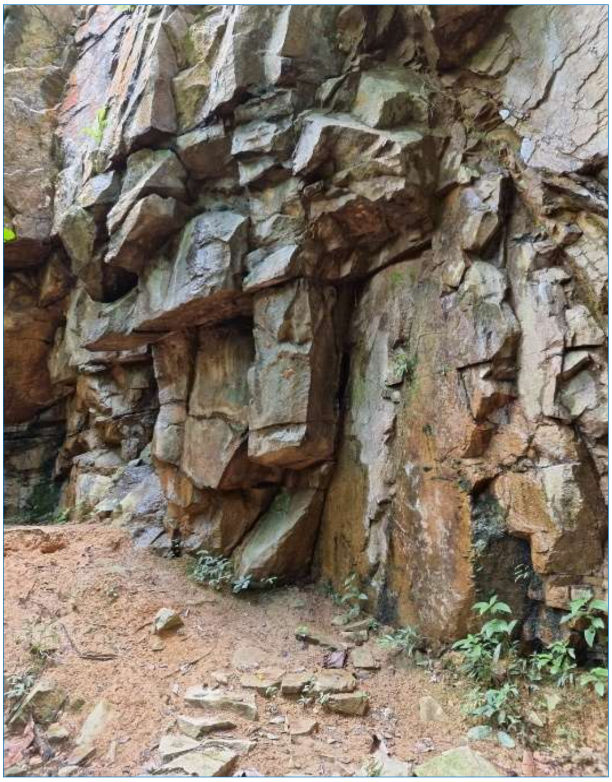

Fig. 13. Damaged rock faces by poor blasting works at project

4.2.1. Assessment Results of Project 2

Almost all rock cliffs were classified as high-risk, with risk levels visually assessed based on the likelihood of rockfall and the presence of unstable geological structures. At location A2, one of 20 specified sites within the former quarry, Q-slope and β determinations are presented in Table 5, with a summary of assessment results and key concerns shown in Table 6.

Fig. 14. a) Observed recent rock fall at Project 2 and b) Observed recent rock fall at Project 2

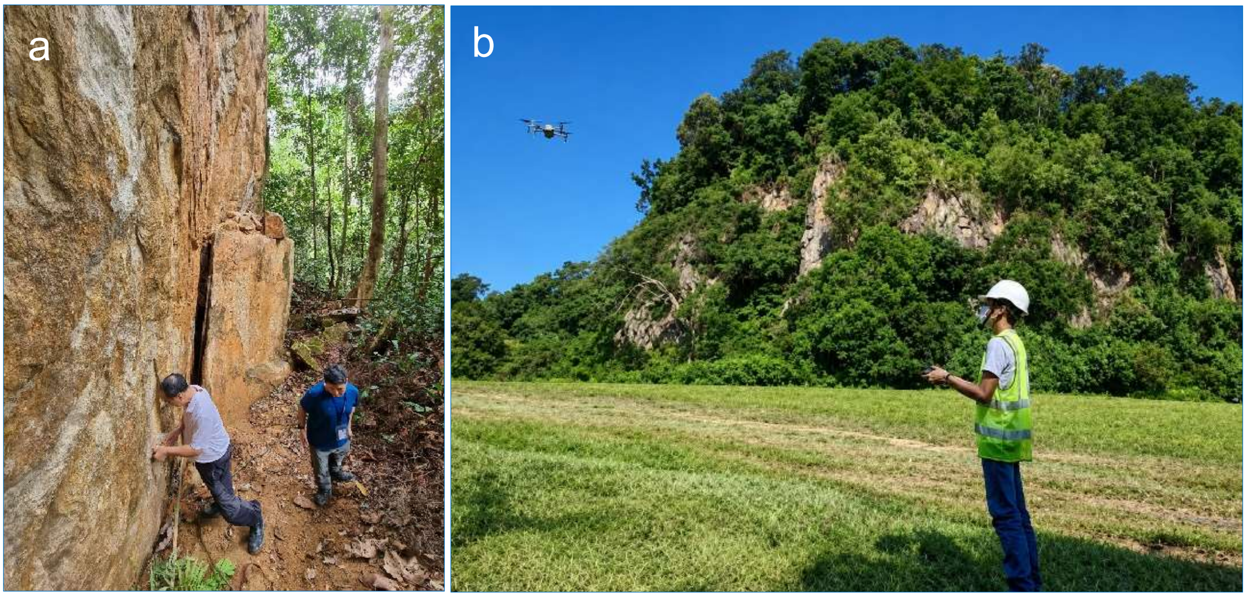

Fig. 15. a) Geological survey along the base of rock cliff and b) Drone imagery for the upper portions of the rock cliff

Two different faces at A2 were assessed, with discontinuity properties included in Table 5. The calculated safe β angle (73°) was lower than the existing cliff slope angle (80°) at one face, indicating instability. As noted in Table 6, the rock cliff was categorized as high-risk due to:

- Highly fractured, closely spaced jointed rock mass
- Overhanging protruding rock blocks
- Loose blocks resulting from sheet joint peel-off
- Toppling failure potential

Supporting photographs are shown in Fig. 16. Assessment results for other rock cliffs in Project 2 similarly indicated high-risk conditions. Due to the significant potential for rockfall, the entire area was deemed unsuitable for mountain hiking.

4.3. Kinematic Analysis of Rock Slopes

Kinematic analysis was carried out applying Dips program (Rocscience Inc., 2025) which is designed for the interactive analysis of orientation based geological data. However, it should be noted that a kinematic analysis only evaluates the geometric feasibility of failure based on discontinuity orientation and friction angle. Therefore, even if the analysis indicates a potential failure mechanism, actual failure may not occur because other factors can contribute to stability, such as joint cohesion, rock bridge strength, and limited joint persistence.

Conversely, slopes that are considered kinematically stable may still fail due to adverse factors such as groundwater pressure, weathering, or seismic loading. In practice, multiple failure modes may occur within the same slope.

Fig. 16 Key Concerns at location A2 (Project 2): a) View of location A2, b) Close-up view of protruding block (top) with highly fractured with closely spaced jointed rock mass (below), c) Highly fractured rock block (top section) with high risk of toppling rock fall potential (below) and d) Loose blocks due to sheet joint peel-off effect with toppling failure potential

4.3.1. Wedge Sliding

The wedge sliding analysis indicates a relatively high proportion of critical intersections, with approximately 17.6% of all joint intersections satisfying the kinematic conditions for wedge failure. This percentage suggests that wedge sliding represents a major potential failure mechanism for the assessed slope orientation (Fig. 17a). The observed wedge type failure in project is shown in Fig. 11d.

4.3.2. Planar Sliding

The planar sliding analysis shows that approximately 10.6% of the discontinuity set falls within the critical planar sliding zone. This relatively high percentage indicates that planar sliding is also a significant concern for slope orientation. In particular, the near-horizontal to low-angle dipping discontinuity planes fall within the daylighting envelope, making them susceptible to planar failure (Fig. 17b). The observed day-lighting joints-controlled failure is depicted in Fig. 11a.

4.3.3. Direct Toppling

The direct toppling analysis identifies a notable toppling potential. The results indicate that approximately 6.7% of the discontinuities satisfy the criteria for direct toppling, while nearly 6.0% satisfy the criteria for oblique toppling (Fig. 17c).

These results suggest that both direct and oblique toppling mechanisms should be considered during stability assessment and slope design. The observed toppling failure is shown in Fig. 11c. The sheeting jointing formed after granitic magma cooling is a kind of toppling failure as shown in Fig. 11b.

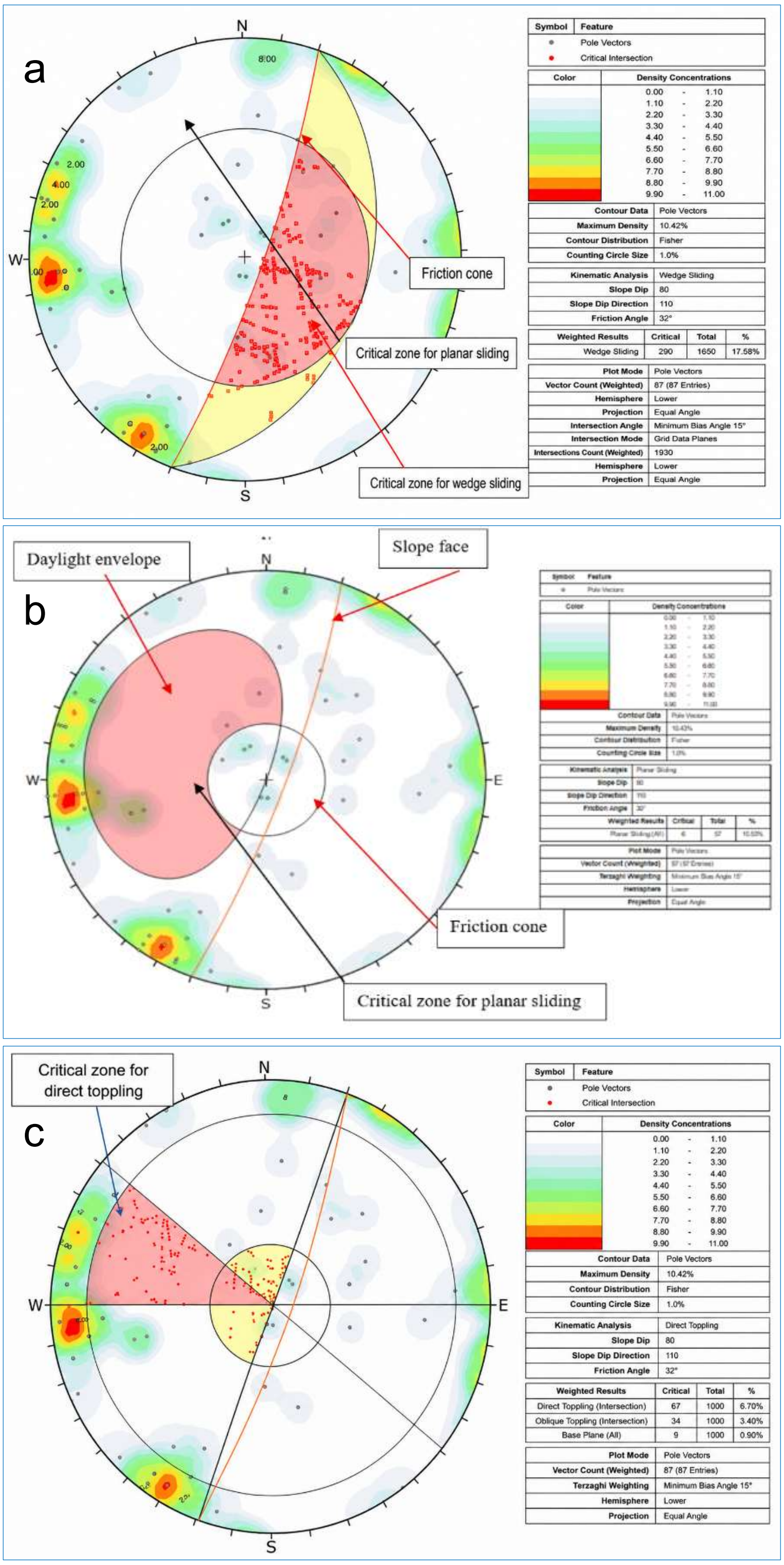

Fig. 17. Kinematic anaysis of rockslopes in Project 2: a) Wedge sliding, b) Planar sliding and c) Direct toppling

ARE THERE POTENTIAL FALLING BLOCKS? **a**	Joint sets (a)		Joint continuity (b)		Faults (c)		Observed overblasting damage (d)		Bench & berm cleanup (e)		Blocks on slopes (f)		Slope height (g)		$A=f[(a+b)+(c+d+e+f)/2]^g$
	0.1	0.5	<1 m	0.6	None	0	Pre-split	-2	Very regular	-3	Many	7-10	<25 m	0.5	
	2	0.5	1-3 m	0.8	Small x 1	0.4	Half-barrels	-0.5	Regular	-1	Several	3-7	50 m	0.8	0<A<10
	3	1	3-10 m	1	Large x 1	1	None	0	Occasional	0	Some	1-3	100 m	1	
	4	2	10-20 m	1.2	2	1.5	Slight	1	Infrequent	1	Few	0.1-1	150 m	1.3	
	>5	7	>20 m	2	>2	2	Excess. overbreak	2.5	Little/none	3	None	0-0.1	>250 m	1.5	A=3.2

ARE THE BLOCKS POTENTIALLY UNSTABLE? **b**	GEOTECHNICAL STUDY + JOINT DATA INTERPRETATION + IN SITU OBSERVATION/RECORDING OF SLOPE LOCAL AND GENERAL INSTABILITY MECHANISMS										
	Mechanism type (observed or estimated)						Affected slope area (%)				
	SIMPLE	B* ("0-8")	COMPLEX	B* ("1-1")	EVOLUTIVE	B* ("1-4")		IN-SITU OBS.	GEOTECH. STUDY	FALLEN BLOCKS AT SLOPE TOE	AVERAGE (correct. B*) P.
	Plane failure	A	Raveling	B	Block topple	C	A	40	40	30	
	Wedge failure		Many block		Flexural topple		B	30	30	30	B=7.0
	Circular failure		Free block		Footwall sice		C	25	25	30	
	B* is a correction factor according to failure mechanism complexity										

Where P is the corrected average for the affected slope area %. Rating (B) is calculated as: $B = 10 \times \left[1-\sqrt[4]{\frac{P}{100}}\right]$ 0<B<10

IS A TRIGGERING EFFECT LIKELY TO PRODUCE INSTABILITY? Triggering Phenomena **c**	Max. 24h rainfall for a 50-year return period (a)		Average 0°C frost-free period (days) (b)		Slope water (c)		Weathering/erosion (d)		Blasting vibration (specific load) (e)		C=a+b+c+d+e
	<50 mm	0.1	>300	0.1	Dry	0	Unweathered	0	<250 g.m/³	0.1	
	50 – 80 mm	0.5	250–300	0.4	Damp	0.3	Slightly weathered	0.3	250–400 g.m/³	0.5	0<C<10
	80 – 110 mm	1.5	200–250	1	Wet	0.7	Weathered	0.7	400–550 g.m/³	1	
	110 – 150 mm	4	150–200	2	Dripping	0.7	Very weathered	1	550–700 g.m/³	1.5	
	>150 mm	6	<150	2.5	Flowing	1	Extremely weathered	1	>700 g.m/³	2	C=4.5

ARE THE BLOCKS LIKELY TO REACH THE MINE BOTTOM? **d**	Bench height (m) Berm/catch-bench width [BW] (m)										General slope dip (a)		Berm conditions & cleanup (b)		Face irregularity (c)		$D=(D_b+a+b+c)^*d$
	5		10		12		15		20								
	BW	D	BW	D	BW	D	BW	D	BW	D							0<D<10
	<1	10	<1	10	<2	10	<3	10	<4	10	40°	+2	Optimal	0	High	+2	
	1.5	7	2	9	3	8	4	9	5	6	48°	+1	Good	+0.5	Medium	+0.5	Estimated probability of block reaching mine bottom
	2	4	3	6	4	5	5	6	6	7.5	56°	+0.5	Limited	+1	Mesh /	ditches	
	2.5	1	4	2	5	2.5	6	3	7.5	2.5	60°	0	Poor	+1.5			
	>3	0	5	0.2	6	1	7	1	9	0.5	72°	-0.5	Very poor	+3	No	1	
			>5.5	0	7.5	0	>8.5	0	10	0	>80°	-1				1	D=9.5

ARE BLOCKS LIKELY TO IMPACT ON WORKERS OR MACHINERY? **e**	Block size (1 falling block) (a_1)		Rock volume (>1 falling blocks) (a_2)		Time spent at slope toe by machinery/ workers (%) (b)	Space occupied by machinery/workers vs. slope length (%) (c)		Position of machinery/ workers in relation to slope toe (d)		E_{mach} = (b/100) * (c-mach/100)a* (a_1 or a_2)*d*10 E_{pers} = (b/100) * (c-pers/100)a* (a_1 or a_2)*d*10
	<0.001 m³	0.9	<0.1 m³	1.5	Days/year	Space occupied by machine vs. slope length (C_{max})	1	Very close (x/H < 10 %)	1	
	0.001–0.1 m³	1	0.1–5 m³	1.5	Shifts/day			Close (x/H < 25 %)	0.5	E=10.-[(10- E_{mach})*(10- E_{pers})/100)
	0.1–1 m³	1.2	5–50 m³	2	Hours/shift	Space occupied by persons (1 m) vs. slope length (C_{pers})	1	Average (x/H < 50 %)	0.1	
	>1 m³	1.5	>50 m³	2.5	16 time under slope			Far (x/H < 100 %)	0.01	0.00025<E<10
								Very far (x/H > 100 %)	0.001	

f SLOPE ROCKFALL HISTORY						
No recorded rockfalls	Very few rockfalls	No data Unreliable observations	Occasional rockfalls	Several rockfalls No accidents	Some rockfalls 1 reported accident	Frequent rockfalls >1 reported accident
0.75	0.9	1.0	1.1	1.2	1.4	1.5

ROFRAQ = (A x B x C x D x E x F) =

ROFRAQ BASIC = (A x B x C x D) = **974**

$ROFRAQ_{pers}$ = (A x B x C x D x E_{pers} x F) =

$ROFRAQ_{mach}$ = (A x B x C x D x E_{mach} x F) =

Estimated probability of an accident due to rockfall occurring on the slope = ROFRAQ / 100,000 =

Preliminary assessment of the quarry face hazard according to ROFRAQ results					
Less than 10	10-25	25-100	100-250	250-1000	More than 1000
VERY LOW RISK	LOW RISK	LOW TO AVERAGE RISK	AVERAGE RISK	HIGH RISK	VERY HIGH RISK
No special measures required	Simple precautionary measures required (inc. regular inspections)	Some simple safety precautions required e.g. avoid traffic under slope toe, scaling, nets, etc.	Important safety measures required. Improve berms and catch-benches, cleanup, bolting, monitoring, etc.	Highly hazardous. Redraft mining plan, enlarge catch-benches, install nets, bolting, monitoring, etc.	Redesign quarry, install meshes, build ditches, etc.

Fig. 18. Rockfall Risk Assessment for Quarry (ROFRAQ) of Project 2, Area 2

4.3.4. Overall Assessment

Based on the kinematic analysis results, wedge sliding presents the highest potential failure risk, followed by planar sliding, while direct and oblique toppling remains noteworthy secondary failure mechanisms. Consequently, all three failure modes should be accounted for in the detailed stability assessment and the development of appropriate slope support and mitigation measures.

5. Rockfall Hazard Assessment at Project 2

The rockfall hazard assessment for Project 2 was conducted using the empirical method Rockfall Risk Assessment for Quarries (ROFRAQ), proposed by Alejano et al. (2008). The method evaluates six parameters as described in section 1.3.

The approach was originally developed from studies of rockfall accidents in active quarries in Spain. To measure the likelihood of rockfall occurrence irrespective of accident outcomes, Alejano et al. (2008) proposed a simplified version of the index, $ROFRAQ_{BASIC}$, based only on the first four parameters (A–D).

For Project 2, the calculation was based on $ROFRAQ_{BASIC}$, as parameters E and F were not applicable to abandoned quarries. This limitation stems from the absence of reliable records of past rockfall incidents. By focusing on $ROFRAQ_{BASIC}$, the assessment remains consistent with available data while acknowledging constraints imposed by incomplete historical information. $ROFRAQ_{BASIC}$ also serves as an indicator of the natural tendency of slopes to release rocks

At Location A2, the rockfall risk assessment (Fig. 18) yielded a score of 974, placing the slope in the High-Risk category (250–1000). Detailed calculations of each sub-rating and rating confirmed a high accident risk.

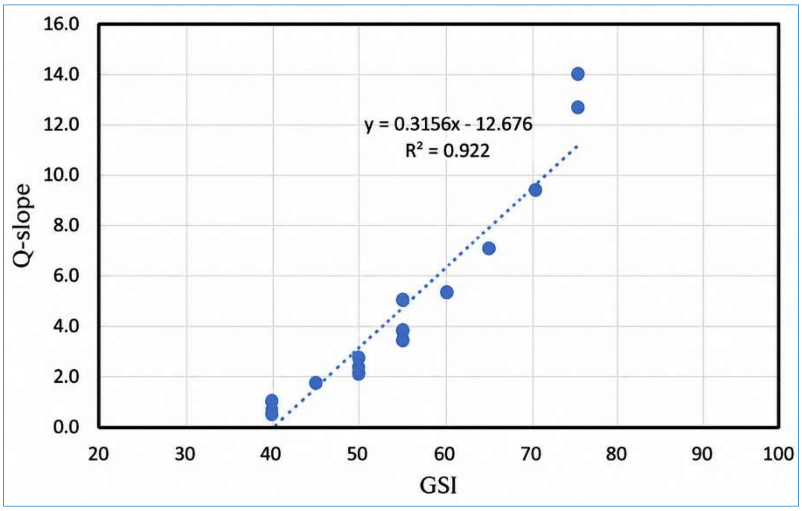

Fig. 19. Correlation of Q-slope Vs Geological Strength Index (GSI)

5.1. Rating A. is there potential falling blocks?

Sub-ratings were derived from joint surveys:

- A(a) = 3 (three joint sets)
- A(b) = 1.2 (joint continuity estimated between 10–20 m)
- A(c) = 0 (no faults observed)
- A(d) = 1.5 (overbreak between slight and excessive)
- A(e) = 0 (face cleanup performed)
- A(f) = 3 (blocks present on slope)
- A(g) = 0.8 (slope height 30–50 m)

After calculation, these values yielded Rating A=3.2 (Fig. 18).

5.2. Rating B. is the Blocks Potentially Unstable?

Joint survey results (Tables 5 and 6) indicated possible kinematic instability mechanisms:

- Toppling (block toppling through vertical to sub-vertical joints)
- Wedge sliding (intersection of joint sets)

Based on continuity, spacing, and slope size, values of 40%, 30%, and 25% were established for wedge failure, local toppling, and slab toppling, respectively. Field observations confirmed similar percentages. Small blocks were observed at the slope toe, with affected areas estimated at 30% for each mechanism. These values yielded Rating B = 7.0 (Fig. 18).

5.3. Rating C. is a Triggering Effect Likely to Produce Instability?

Scores were assigned as follows:

- C(a) = 4 (rainfall intensity)
- C(b) = 0.1 (frost-free period)
- C(c) = 0.1 (water effects)
- C(d) = 0.3 (weathering effects)
- C(e) = 0 (no blasting activity in >20 years)

The calculated value was Rating C = 4.5 (Fig. 18).

5.4. Rating D. is Blocks Likely to Reach the Mine Bottom?

As no catch benches were present, all falling blocks would reach the quarry bottom. For benches >20 m and berms <4 m wide, the combined sub-rating (Db + Da) was 10. With a slope correction of –0.5, the final value was Rating D = 9.5 (Fig. 18).

5.5. ROFRAQ$_{BASIC}$ Value

The ROFRAQ$_{BASIC}$ index was calculated as:

$$ROFRAQ_{\ BASIC} = A \times B \times C \times D = 974 \tag{3}$$

This value falls within the High-Risk category, consistent with in-situ observations (Tables 5 and 6). Although developed for temperate climates, the probabilistic framework of ROFRAQ is adaptable to tropical environments such as Singapore, provided local climatic influences (e.g., rainfall intensity, seasonal variability) are considered.

Table 5. Q-slope and β determination of quarry wall rock mass (Location A2, Project 2)

Slope stability Analysis			Location – A2		
RQD	90	70			
Jn	6	6	2 Major sets + 1 Minor set		
Jr	3	3	Rough / ~~smooth~~ / ~~slicken-sided~~ / planar / undulating		
Ja	1	1	~~Unaltered~~ / ~~altered~~ / surface staining / clay filling & moss)		
O factor	1	0.75	Favourable / ~~unfavourable~~ / ~~likely to fail~~		
Jwice	0.7	0.5	Stable / ~~unstable~~ / competent / ~~incompetent~~		
SRFa	2.5	5	Slight loosening / loose blocks		
SRFb	1	1	Moderate / ~~high stress~~		
SRFc	1	1	Major discontinuity with no clay / ~~with clay~~		
Qslope	12.60	2.63			
β	87	73			
Current slope face (angle / alignment direction)				80	
Significant features on slope surface (water flowing)				dripping when rain	
			Joint Data (dip amount / direction)		
J1	90/030-210	**J2**	90/010-190	**J3**	90/70-250
J4	40/250	**J5**	90/110-290	**J6**	82/090
Joint persistence (in m)		Good, bottom to top of slope			
Joint spacing (in m)		2.5 cm to > 20 cm			
Joint aperture (in mm)		close to 5 cm aperture			
Significant geological structures					
Obvious protruding hanging rock block	Daylighting joint below hanging rock block				
Remarks					
Potential to rockfall			**High risk**		

Table 6. Summary of assessment of location A2 (Project 2)

Parameter	Description
Location	A2
Key concerns	-Highly fractured with closely spaced jointed rock mass -Overhang protruding loose blocks -Loose blocks due to sheet joint peel-off effect (Toppling Failure) -Wedge shaped failure plane
Additional visual observation	-Vegetation above study area -Noticed multiple rock debris at bottom (consistent rock chipping off rock slope) -No continuous heavy water flowing (only water dripping)
Recent (failures)	No major impact observed during study period
Risk factor	High Risk

6. Correlation between Q-slope and Geological Strength Index (GSI)

Q-slope and Q-slope' have been correlated with other rock mass classification systems, including:

- BQ method (Song et al., 2019)
- Continuous Slope Mass Rating (CSMR) (Siddique et al., 2020)
- Geological Strength Index (GSI) (Narimani et al., 2023)
- Rockfall Hazard Rating System (RHRS) (Saito de Paula et al., 2019)
- Slope Mass Rating (SMR) (Jorda-Bordehore et al., 2018; Azarafza et al., 2022)
- Slope Stability Assessment Methodology (SSAM) (Bar and McQuillan, 2021)

The Geological Strength Index (GSI), introduced by Hoek et al. (1992) and further developed by Hoek (1994, 1995), is widely used to characterize the mechanical behaviour of jointed and fractured rock masses. It provides a reduction factor to estimate rock mass strength when combined with intact rock properties under varying geological conditions. In this research, the correlation between Q-slope and GSI for granitic rock mass from project 2 was conducted and results as follows (Fig. 19).

$$Q\text{-}slope = 0.3156\ (GSI) - 12.67 \tag{4}$$

$$R^2 = 0.922 \tag{5}$$

Fig. 20 explains how to determine GSI at some areas in Project 2 with photographic evidence. It was not possible to establish a reliable correlation between modified Q-slope (Q-slope') and GSI, as attempted by Narimani et al. (2023). The authors argue that correlations should be developed using the original Q-slope system, which accounts for environmental and stress conditions. This research represents the first application of the Q-slope method in Singapore, and the findings are expected to contribute to the development of local correlations. Continued refinement and advancement of the Q-slope approach for rock slope engineering in Singapore are strongly encouraged.

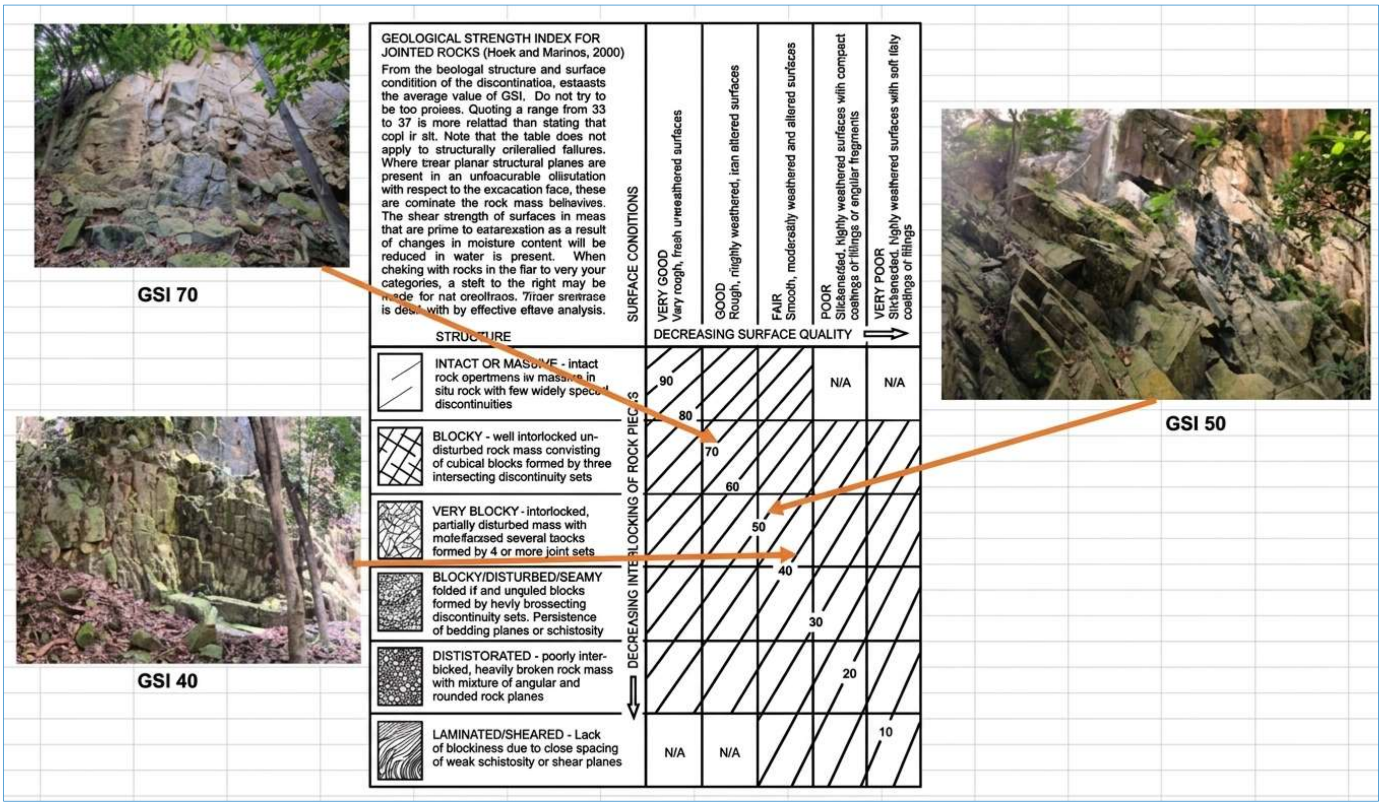

Fig. 20. Determination of GSI at some areas in Project 2

7. Conclusion

This study constitutes the first documented application of the Q-slope method in Singapore, marking an important step toward establishing localized correlations between Q-slope values and the Geological Strength Index (GSI) and advancing slope stability assessment practices in tropical quarry environments. This study successfully demonstrates the first application of the Q-slope and ROFRAQ methodologies to the weathered granitic slopes of Singapore. Our findings indicate a strong empirical correlation between Q-slope and the Geological Strength Index (GSI) for the Bukit Timah Centre Granite (R^2 = 0.922), providing a new predictive tool for engineering geologists in tropical regions. While traditional kinematic analysis identifies potential wedge and planar failures, the integration of Q-slope allows for a more nuanced assessment of long-term stable slope angles in highly weathered rock masses. Furthermore, the application of the ROFRAQ system provides a critical safety framework for urban redevelopment. By quantifying rockfall risks, we have established evidence-based stand-off distances that safeguard public infrastructure while optimizing land use in a land-scarce environment. These results emphasize that geological assessments in tropical climates must account for specific weathering profiles and high-intensity rainfall, offering a methodology that can be adapted for similar geological settings globally. Future research will focus on expanding this dataset to include a wider range of tropical rock types to further refine these empirical correlations.

Acknowledgement

The authors wish to thank the anonymous reviewers for their valuable time and effort on this manuscript.

Author contributions

Kar Winn: Field investigation of both projects, Writing-Reviewing and Editing, Chow Weng Lee: Field investigation of project 1, Writing-Reviewing and Editing, Ong Perng Fey: Field investigation of project 2, Writing-Reviewing and Editing, Htet Aung Linn: Field investigation and supervision of both projects.

Data Availability

The data used to support the findings of this study are included in this article.

Declarations

Conflict of interest: The authors declare that they have no conflict of interest. No external funding was received for undertaking this study.

Funding

This research did not receive any specific grant from funding agencies in the public, commercial, or not-for-profit sectors.

References

Alejano, L.R., Stockhausen, H.W., Alonson, E., Bastante, F.G., Oyanguren, P.R., 2008. ROFRAQ: A statistic based empirical method for assessing accident risk from rockfalls in quarries. International Journal of Rock Mechanics and Mining Sciences 45 (8), 1252-1272. https://doi.org/10.1016/j.ijrmms.2008.01.003.

Azarafza, M., Nanehkaran, Y.A., Rajabion, L., Akgun, H., Rahnamarad, J., Derakhshani, R., Raoof, A., 2020. Application of the modified Q-slope classification system for sedimentary rock slope stability assessment in Iran. Engineering Geology 264, 105-349. https://doi.org/10.1016/j.enggeo.2019.105349.

Azarafz, M., Kockar, M.K., Zhu, H.H., 2022. Correlations of SMR-Q-slope data in stability classification of discontinuous rock slope: a modified relationship considering the Iranian data. Geotechnical and Geological Engineering 40, 1751-1764. https://doi.org/10.1007/s10706-021-01991-w.

BCA, 2021. Building and Construction Authority Singapore, 2021. Singapore Geology, 173 pp, ISBN 978-0-85272-791-1.

Bar, N., Barton, N.R., 2016. Empirical slope design for hard and soft rocks using Q-slope. ARMA 16-384, Symposium of American Rock Mechanics Society.

Bar, N., Barton, N., 2017. The Q-Slope Method for Rock Slope Engineering. Rock Mechanics & Rock Engineering 50 (12), 3307-3322. https://doi.org/10.1007/s00603-017-1305-0.

Bar, N., Barton, N., 2018a. Rock slope design using Q-slope and geophysical survey data. Periodica Polytechnica Civil Engineering 62 (4), 893-900. https://doi.org/10.3311/PPci.12287.

Bar, N., Barton, N., 2018b. Q-Slope: An Empirical Rock Slope Engineering Approach in Australia. Australian Geomechanics Journal 53 (4), 73-86.

Bar, N., Barton, N., 2025. Q-slope: Rock Slope Engineering 10 years on. Rock Mechanics and Rock Engineering 58, 11453-11474. https://doi.org/10.1007/s00603-024-04064-5.

Bar, N., Mc Quillan, A., 2021. Q-slope and SSAM applied to excavated coal mine slopes. MethodsX 8 (101191). https://doi.org/10.1016/j.mex.2020.101191.

Barton, N., Lien, R., Lunde, J., 1974. Engineering classification of rock masses for the design of tunnel support. Rock Mechanics 6, 189-236. https://doi.org/10.1007/BF01239496.

Barton, N., Grimstad, E., 2014. Forty years with the Q-system in Norway and abroad. Fjellsprengningsteknikk, Bergmekanikk/Geoteknikk 2014, 4.1–4.25. Norsk Fjellteknisk Forening, Oslo, Norway.

Barton, N., Bar, N., 2015. Introducing the Q-slope method and its intended use within civil and mining engineering Case Studys. In: Schubert & Kluckner (ed), Future Development of Rock Mechanics: Proceedings of the ISRM Reg. Symp. Eurock 2015 & 64th Geomechanics Colloquium, Salzburg, 7-10 October 2015, pp 157-162.

Barton, N., Shen, B., Bar, N., 2018. Limited heights of vertical cliffs and mountain walls linked to fracturing in deep tunnels – Q-slope application if jointed slopes. Proc. XIX Congresso Brasileiro de Mecânica dos Solos e Engenharia Geotécnica Geotecnia e Desenvolvimento Urbano: COBRAMSEG 2018, Salvador, 28 August – 1 September 2018, ABMS, 13p.

Barton, N., Bar, N., 2019. The Q-slope method for rock slope engineering in faulted rocks and fault zones. In: Fontura et al. (eds), Rock mechanics for natural resources and infrastructure development, Proceedings of the 14th international congress on rock mechanics and rock engineerinh, Foz do Iguassu, 13-18 September 2019, pp 3424-3432.

Bieniawski, Z.T., 1976. Rock mass classification in rock engineering. In: Bieniawski (ed), Exploration for rock engineering: Proceedings of the symposium, Balkema, Cape Town, pp. 97-106.

Bieniawski, Z.T., 1989. Engineering rock mass classifications: a complete manual for engineers and geologists in mining, civil and petroleum engineering. Wiley, New York. P272.

Gupta, K., Gupta, S., Haris, P.M., Siddque, T., 2025. A multi-platform tool for modified Q-slope assessment in rock engineering: validation from the Himalayas. Geotechnical and Geological Engineering 43, 462. https://doi.org/10.1007/s10706-025-03440-4.

Hoek, E., Wood, D., Shah S., 1992. A modified Hoek-Brown criterion for jointed rock masses. Proc. Rock characterization, symp. Intl. Soc. Rock Mech.: Eurock 1992, (Ed. J.A. Hudson), 209-214. London: Brit. Geol. Soc.

Hoek, E., 1994. Strength of rock and rock masses. ISRM News Journal 2 (2), 4-16.

Hoek, E., Kaiser, P.K., Bawden, W.F., 1995. Support of underground excavations in hard rock. Rotterdam: Balkema, Rotterdam.

Jorda-Bordehore, L., Bar, N., Cano, M., Riquelme, A., Tomas, R., 2018. Stability assessment of rock slopes using empirical approaches: comparison between Slope Mass Rating and Q-slope. In: Proceedings of XIV Congreso International de Energiay Recursos Minerales and Slope Stability 2018, 10-13 April 2018, Seville, Spain, p 5 ionship considering the Iranian data. Geotechnical and Geological Engineering 40, 1751-1764. https://doi.org/10.1007/s10706-021-01991-w.

Kalpakci, V., Ozturk, S., Topal, T., Huvaj, N., 2016. Investigation of rock slope stability for an abandoned limestone quarry in Konya Turkey. Landslides and engineered slopes. Experience, Theory and Practice – Aversa et al. (Eds) Associazione Geotecnica Italiana, Rome, Italy, ISBN 978-1-138-02988-0.

Kouhdaragh, M., Azarafza, M., Derakhshani, R., 2022. A Q-slope based empirical method to stability assessment of mountain rock slopes in multiple faults zone: a case for North of Tabriz. MethodsX 9, 101718. https://doi.org/10.1016/j.mex.2022.101718.

Kolano, M., Cala, M., Stopkowicz, A., Olchowy P., Wendorff, M., 2015. Stability assessment of rock slopes in the former quarry of Wojciech Bednarski Park in Krakow – A case study. Applied Science 15, 7197. https://doi.org/10.3390/app15137197.

Laubscher, D.H., 1977. Geomechanics classification of jointed rock masses – mining applications. Trans Inst Metall Sect A Min Ind 93: A1-A8.

Laubscher, D.H., Jakubec, J., 2001. The MRMR rock mass classification for jointed rock masses, In: Hustrulid, Bullock (eds) Underground mining methods: engineering fundamentals and international case studies. AIME, New York, pp 474-481.

Mao, Y., Chen, L., Nanehkaran, Y.A., 2023. Fuzzy-based intelligent model for rapid rock slope stability analysis using Q-slope. Water 15 (16), 2949. https://doi.org/10.3390/w15162949.

Narimani, S., Davarpanah S.M., Bar, N., Torok, A., Vasarhelyi, B., 2023. Geological strength index relationships with the Q-system and Q-slope. Sustainability 15, 11233. https://doi.org/10.3390/su151411233.

Rocscience Inc., 2025. DIPS: Interactive Analysis of Orientation-Based Geological Data [Computer software]. Rocscience Inc., Toronto, Canada.

Romana, M., 1985. New adjustment ratings for application of Bieniawski classification to slopes. In: Proceedings of the ISRM international symposium in role of rock mechanics in excavations for mining and civil works, Zacatecas, pp. 49-53.

Romana M., 1995. The geomechanical classification SMR for slope correction. In: Proceedings of the 8th ISRM congress on Rock Mechanics 3, Tokyo, 25-29 September 1995, pp 1085-1092.

Saito, de Paula, M., Maion, A.V., Campanha, G.A.G., Castilho, L.M.N., Cunha, M.A., 2020. Q-slope and RHRS for the evaluation of highway rock slopes - Serra do Mar, Brazzil. In: Fontura et al. (eds), Rock mechanics for natural resources and infrastructure development, Proceedings of the 14th International Congress on Rock Mechanics & Rock Engg, Foz do Iguassu, 13-18 September 2019, p8

Song, Y., Xue, H., Meng, X., 2019. Evaluation method of slope stability based on the Q-slope system and BQ method. Bulletin of Engineering Geology and the Environment 78, 4865-4873. https://doi.org/10.1007/s10064-019-01459-5.

Siddique, T., Pradhan, S.P., Vishal, V., Singh, T.N., 2020. Applicability of Q-slope method in the Himalayan Road cut rock slopes and its comparison with CSMR. Rock Mechanics and Rock Engineering 53, 4509-4522. https://dot.org/10.1007/s00603-020-02176-2.

Tomas, R., Delgado, J., Seron, J.B., 2007. Modification of slope mass rating (SMR) by continuous functions. International Journal of Rock Mechanics and Mining Sciences 44, (7): 1062-1069. https://doi.org/10.1016/j.ijrmms.2007.02.004.

Tomas, R., Cuenca, A., Cano, M., Garcia-Barba, J., 2012. A graphical approach for slope mass rating (SMR). Eng Geol 124: 67-76. https://doi.org/10.1016/j.enggeo.2011.10.004.

Winn, K., Lee, C.W., Linn, H.A., 2022. Rock slope stability analysis of abandoned quarry wall applying Q-slope method: Singapore case study (AUSROCK Conference, Nov-Dec 2022, Melbourne, Australia).